Indian J. Phys. **72A** (6), 547–566 (1998)

IJP A
— an international journal

Structure functions—selected topics

D K Choudhury
Department of Physics, Gauhati University,
Guwahati-781 014, Assam, India

Abstract : We summarise a few topics of DIS like double asymptotic scaling, and spin and diffractive structure.

Keywords : Structure function, HERA, Low X

PACS Nos. : 13.88.+e, 13.60.Hb, 12.38.Bx, 12.38.Lg

1. Introduction

Deep Inelastic lepton scattering experiments have made very important contributions to the understanding of the structure of matter. The long tradition of experiments of deep inelastic scattering started with the experiment at the linear accelerator at SLAC in 1968, where an approximate scaling of the nucleon structure function in a dimensionless variable x gave first evidence for scattering on charged pointlike constituents of the nucleon. In the 70's and 80's, beam energies upto several hundred GeV become available and allowed to measure precisely the logarithmic scaling violation in the structure functions which become instrumental for testing QCD. In 1992, the ep collider HERA was put in operation, where centre-of-mass energy of 300 GeV can be reached [1] compared to about 30 GeV in fixed target experiment. This makes it possible to explore a new domain in x and Q^2. Specially low x regime ($x \leq 10^{-4}$) has received intense theoretical and experimental attention [2]. Similarly, probing the structure of the Pomeron at HERA [3] through diffractive structure function has opened a new dimension in the physics of deep inelastic scattering. In the spin physics on the other hand, new information on g_2 has been reported [4,5].

The present talk deals with following few selected topics of deep inelastic scattering :

- Double asymptotic scaling
- Gluon and longitudinal structure functions at low x

- Diffractive structure functions
- Spin structure functions.

2. Double asymptotic scaling

As early as 1974, it was shown that with reasonable boundary conditions [6], perturbative QCD predicts a universal growth in the gluon momentum density at large t ($t = \ln \frac{Q^2}{\Lambda^2}$) and small x faster than any power of $\ln \frac{1}{x}$ but slower than any inverse power of x. More recently, Ball and Forte [7] brought this perturbative to the phenomenological front. They have recast the result of reference [6] in two asymptotic variables

$$\sigma = \sqrt{\ln \frac{x_0}{x} \ln \frac{t}{t_0}}, \quad \rho = \sqrt{\frac{\ln (x_0/x)}{\ln (t/t_0)}}. \tag{1}$$

HERA [8] provides excellent agreement with both the scaling predictions and confirm the perturbative results [6]. The asymptotic behaviour of $F_2(\sigma, \rho)$ is then

$$F_2(\sigma, \rho) \sim Nf\left(\frac{\gamma}{\rho}\right)\frac{\gamma}{\rho}\frac{1}{\sqrt{\gamma\rho}} \exp\left[2\gamma\sigma - \delta\left(\frac{\sigma}{\rho}\right)\right]\left[1 + O\left(\frac{1}{\sigma}\right)\right] \tag{2}$$

where
$$\gamma = 2\sqrt{\frac{N_c}{\beta_0}}, \quad \beta_0 = \frac{11}{3}N_c - \frac{2}{3}n_f, \tag{3}$$

and
$$\delta = \frac{\left(1 + \frac{2n_f}{11N_c^3}\right)}{\left(1 - \frac{2n_f}{11N_c}\right)\left(\frac{N_c}{3}\right)}. \tag{4}$$

N_c and n_f being the number of colours and flavours respectively. The unknown function f, which depends on the details of the starting distribution tends to one for sufficiently small values of its argument. N is an *a priori* undetermined normalisation factor. For $n_f = 4$ and $N_c = 3$, $\delta \approx 1.36$.

In order to test this prediction, data [9] are presented in the variables σ and ρ, taking the boundary conditions to be $x_0 = 0.1$ and $Q_0^2 = 1$ GeV^2, and $\Lambda_{\overline{\text{LO}}}^{(4)} = 185$ MeV. The measured value of F_2 are rescaled by

$$R_{F'}(\sigma, \rho) = 8.1 \exp\left[\delta\frac{\sigma}{\rho} + \frac{1}{2}\ln(\sigma) + \ln\left(\frac{\rho}{\gamma}\right)\right] \tag{5}$$

to remove the part of the leading subasymptotic behaviour which can be calculated in a model independent way; $\ln(R_{F'}F_2)$ is then predicted to rise linearly with σ and with a slope 2γ.

Figure (1a) shows such a linear rise. A fit to the data gives the value of $2.22 \pm 0.04 \pm 0.10$ for the slope. The result agrees well with the prediction of the slope $2\gamma = 2.4$ for four flavours. Figure (1a) contains data with $\rho^2 > 1.5$ only.

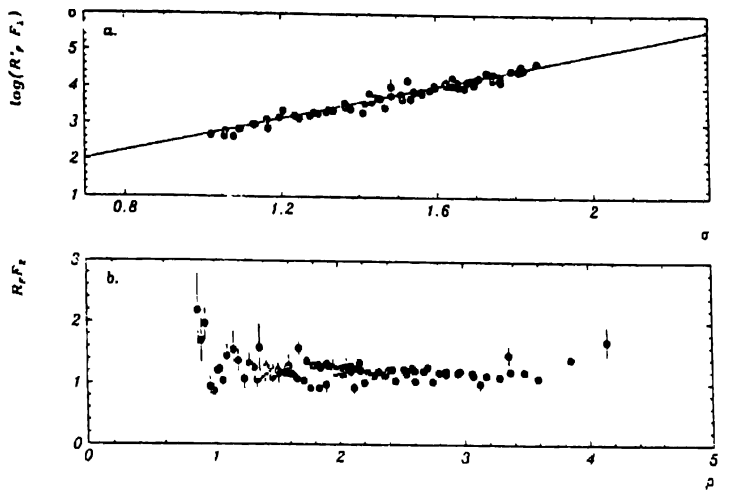

Figure 1. The rescaled structure functions $\log(R'_F F_2)$ and $R_F F_2$ plotted *versus* the variables σ and ρ defined in the text. Only data with $\rho^2 > 1.5$ are shown in (a).

Scaling in ρ can be shown by multiplying F_2 by the factor

$$R_F = R_F \cdot e^{-2\gamma\sigma}. \tag{6}$$

This rescaled structure function should scale in both σ and ρ when both lie in the asymptotic regions. Figure (1b) shows the scaling in ρ which sets in for $\rho \geq 1.2$.

The prediction for $R_F F_2$ as a function of ρ only depends on the gluon density at Q_0^2. While for a soft starting gluon distribution, scaling for the full asymptotic region is predicted, a hard gluon input would lead to scaling violation at high ρ [7]. The data shown in Figure [1(a, b)] are well described by the asymptotic behaviour derived from soft boundary conditions.

More recently, Ball and Forte [10] developed the double scaling formalism with NLO effects. In this case, σ and ρ are defined as

$$\sigma = \sqrt{\ln\left(\frac{x_0}{x}\right) \ln \frac{\alpha_s(Q_0^2)}{\alpha_s(Q^2)}}, \tag{7}$$

$$\rho = \sqrt{\frac{\ln(x_0/x)}{\ln \dfrac{\alpha_s(Q_0^2)}{\alpha_s(Q^2)}}}, \tag{8}$$

where $\alpha_s(Q^2)$ is to be evaluated at the two loop level.

$$\alpha_s(Q^2) = \frac{4\pi}{\beta_0 \ln\frac{Q^2}{\Lambda^2}}\left(1 - \frac{\beta_1}{\beta_0^2}\frac{\ln\ln\frac{Q^2}{\Lambda^2}}{\ln\frac{Q^2}{\Lambda^2}}\right) \tag{9}$$

with $\beta_1 = 102 - \frac{38}{3}n_f$.

In order to obtain the structure function within the NLO DAS formalism, one defines besides the usual logarithmic QCD evolution variables $t = \ln(\frac{Q^2}{\Lambda^2})$ and $\xi = \ln(\frac{1}{x})$, the evolution length T of $\alpha_s(Q^2)$ from a starting point Q_0^2 to Q^2

$$T = \ln\left(\frac{\alpha_s(Q_0^2)}{\alpha_s(Q^2)}\right). \tag{10}$$

To leading order, T is simply $\ln(\frac{t}{t_0})$.

For large t and ξ and an $F_2(x, Q^2)$ which at Q_0^2 is not too singular in x, the NLO double asymptotic expression for $F_2(x, Q^2)$ is [10]

$$F_2 \sim N_F(1 - f_{\text{NLO}})\exp\left[2\gamma\sqrt{\xi T} - \delta T + \frac{1}{4}\ln T - \frac{3}{4}\ln\xi\right]. \tag{11}$$

The normalisation coefficient N_F is

$$N_F = \frac{\sqrt{\gamma}}{\pi}\frac{5n_f}{324}. \tag{12}$$

For $n_f = 4$ and $N_c = 3$, it gives $\gamma = 516$, $\delta = \frac{4}{3}$ and $N_F = 0.038$.

The NLO correction term f_{NLO} is

$$f_{\text{NLO}} = \frac{\sqrt{\xi/T}}{2\pi\gamma}\left[\epsilon\left(\alpha_s(Q_0^2) - \alpha_s(Q^2)\right) - 13\alpha_s(Q^2)\right] \tag{13}$$

and

$$\epsilon = \left(\frac{206n_f}{27} + \frac{6\beta_1}{\beta_0}\right). \tag{14}$$

The leading order formula is recovered by setting $f_{\text{NLO}} = 0$ and $\beta_1 = 0$. Defining leading exponent as

$$\lambda\xi = 2\gamma\sqrt{\xi T} \tag{15}$$

and the subleading term as

$$\alpha = -\delta T + \frac{1}{4}\ln T - \frac{3}{4}\ln\xi \tag{16}$$

one rewrites F_2 as

$$F_2 \sim x^{-\lambda}e^{\alpha} \tag{17}$$

The leading term in the double asymptotic formula for F_2 corresponds to the double leading log approximation DLL [11] of the DGLAP equations [12]. It generates the growth of the structure function with falling x proportional to λ

$$\lambda \sim 2\gamma \sqrt{\frac{\ln t}{\ln \frac{1}{x}}}. \tag{18}$$

The subleading term also falls with x but slower than the leading term growth.

This formulation has been used recently by H1 Collaboration [13].

The value $x_0 = 0.1$ as suggested earlier [7,9] was found to be a good choice while Q_0^2 is set at $Q_0^2 = 2.5$ GeV^2. To visualise the double scaling, it was proposed to rescale F_2 with factors R_F' and R_F related by (6) but the explicit term is modified as

$$R_F(\sigma,\rho) = \frac{8.1 \exp\left[-2\gamma\sigma + \omega\frac{\sigma}{\rho} + \frac{1}{2}\ln(\gamma\sigma) + \ln\left(\frac{\rho}{\gamma}\right)\right]}{\xi_F}, \tag{19}$$

where
$$\xi_F = 1 + \left[(\xi_1 + \xi_2)\alpha_s(Q^2) - \xi_1\alpha_s\left(Q_0^2\right)\left(\frac{\rho}{2\pi\gamma}\right)\right], \tag{20}$$

$$\xi_1 = \frac{\frac{206}{27}n_f + \frac{6\beta_1}{\beta_0}}{\beta_0}; \qquad \xi_2 = 13, \tag{21}$$

$$\omega = \frac{11 + \frac{2}{27}n_f}{\beta_0}. \tag{22}$$

Figure (2a) shows $R_F F_2$ *versus* ρ to the data with $Q^2 \geq 3.5$ GeV^2. The value of Λ for four flavours is chosen to be $\Lambda = 263$ MeV. Approximate scaling is observed for $Q^2 \geq 5$ GeV^2 and $\rho \geq 2$. At high ρ, the low Q^2 data tend to violate the scaling behaviour which is clearly seen from the data at 3.5 GeV^2.

In Figure (2b), $\ln R_F' F_2$ is shown for $\rho \geq 2$ and $Q^2 \geq 5$ GeV^2 as a function of σ. The data exhibits the linear growth with σ. A linear fit to the data gives a value for the slope to be $2.50 \pm 0.02 \pm 0.06$ ($2.57 \pm 0.05 \pm 0.06$) for $Q^2 < 15$ GeV^2 ($Q^2 > 35$ GeV^2) and 4 (5) flavours. The results are in agreement with the QCD prediction : 2.4 and 2.5 for $n_f = 4, 5$ respectively. Compared to the result presented in references [7,9], the extraction based on the 2-loop formalism [10] is in better agreement with QCD expectation.

One can therefore conclude that low x, low Q^2 measurements for $Q^2 \geq 5$ GeV^2 show scaling in ρ and σ. The double asymptotic scaling is a dominant feature of F_2 in this region.

In a recent analysis [14], Λ and α_s are determined by fitting the expression (9) for $F_2(x, Q^2)$ to the latest measurement of the proton structure function by the H1

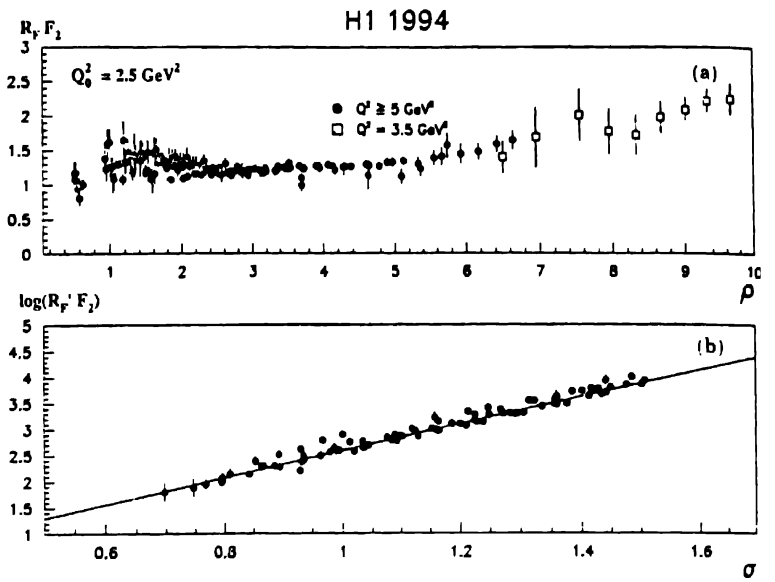

Figure 2. The rescaled structure functions (a) $R_F F_2$ *versus* ρ and (b) $\log(R_F F_2)$ *versus* σ using NLO-DAS formalism. Only data with $Q^2 \geq 5$ GeV^2 and $\rho > 2$ are shown in (b).

experiment [13] at HERA yielding $\Lambda \sim 248$ MeV, $\alpha_s(m_Z^2) = 0.113 \pm 0.002$ (*stat*) ± 0.007 (*syst*) at $Q^2 = 1.12$ GeV^2. The authors also attempt a QCD inspired parametrization with leading exponent of (9):

$$F_2(x, Q^2) = N_f\, x^{-\gamma\sqrt{T/\xi}} \tag{23}$$

with $n_f = 4$.

The NLO double asymptotic expression (11) and the modified DLL form (23) are shown in Figure 3. The modified DLL form (23) is fitted with two parameters $Q_0^2 = 0.365 \pm 0.026$ (*stat*) ± 0.048 (*syst*) GeV^2 and $\Lambda = 243 \pm 13 \pm 23$ MeV.

Let us conclude this subsection with a caution. In a recent work, Buchmüller and D Haidt [15] obtains an equally good fit of the recent data [16] with a simple double logarithmic form

$$F_2(x, Q^2) = a + m \ln\frac{Q^2}{Q_0^2} \ln\frac{x_0}{x} \tag{24}$$

with $$a = 0.078,\ m = 0.364,\ x_0 = 0.074,\ Q_0^2 = 0.5\ \text{GeV}^2. \tag{25}$$

Hence the characteristic feature of double asymptotic scaling, a growth stronger than any power of $\ln\frac{1}{x}$, cannot be confirmed from the present HERA data. This more singular

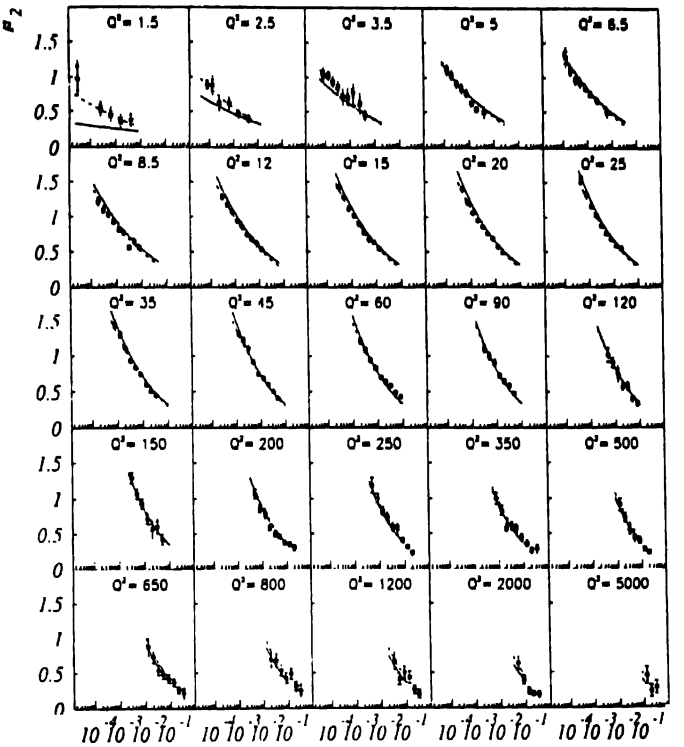

Figure 3. The proton structure function $F_2(x,Q^2)$ as measured by the H1 experiment at HERA together with a fit to the NLO double asymptotic expression (11) (full line) for $Q^2 > 5$ GeV^2 and with a fit to the modified DLL expression (23) (dashed line) in the full Q^2 range.

behaviour should become visible, if at given Q^2, the range in x is extended at least by one order of magnitude. In that small x range, the more singular, BFKL [17] power behaviour may also perhaps be distinguished. This corresponds to an increase in the centre-of-mass energy squared by one order of magnitude, which could be reached at future colliders, such as LEP ⊗ LHC or at a 500 GeV^2 Linear Collider⊗ HERA.

3. Measuring Gluon and longitudinal structure functions

3.1. Approximate relation between gluon and longitudinal structure functions :

In leading order in α_s, the longitudinal structure function $F_L(x, Q^2)$ is given by [12]

$$F_L(x,Q^2) = \frac{\alpha_s(Q^2)}{2\pi}\left[\frac{8}{3}\int_x^1 \frac{dy}{y}\left(\frac{x}{y}\right)^2 F_2(y,Q^2) + 2\sum e_q^2 \int_x^1 \frac{dy}{y}\left(\frac{x}{y}\right)^2\left(1-\frac{x}{y}\right) y G(y,Q^2)\right] \tag{26}$$

where e_q^2 denotes the charge squared of the partons.

In the low x limit, it yields [18] for four active flavours

$$xG(x,Q^2) = \frac{3}{5}\,5.8\left[\frac{3\pi}{4\alpha_s}F_L(0.417x,Q^2) - \frac{1}{1.97}F_L(0.75x,Q^2)\right]. \quad (27)$$

Neglecting the quark contribution [18], one obtains

$$F_L(0.47x,Q^2) = \frac{2\alpha_s}{3\pi}\frac{1}{1.74}xG(x,Q^2), \quad (28)$$

which directly relates gluon density to longitudinal structure function. NLO correction to (28) has been reported by Zilstra and Van Neerven [19]. Recently [20] (28) has been used to test the gluon density with factorisable x and Q^2 dependence by predicting the longitudinal structure function. Such a factorisable gluon has the universal limiting behaviour at low x

$$G(x,t) = G(x,t_0)\left(\frac{t}{t_0}\right)^{\frac{36}{25}\ln\left(\frac{1}{x}\right)} \quad (29)$$

In Figure 4, the predictions of F_L using (29) are compared with those obtained with collinear [19] and k_T factorisation approach [21] at $Q^2 = 20$ GeV^2. Prediction of (29) are

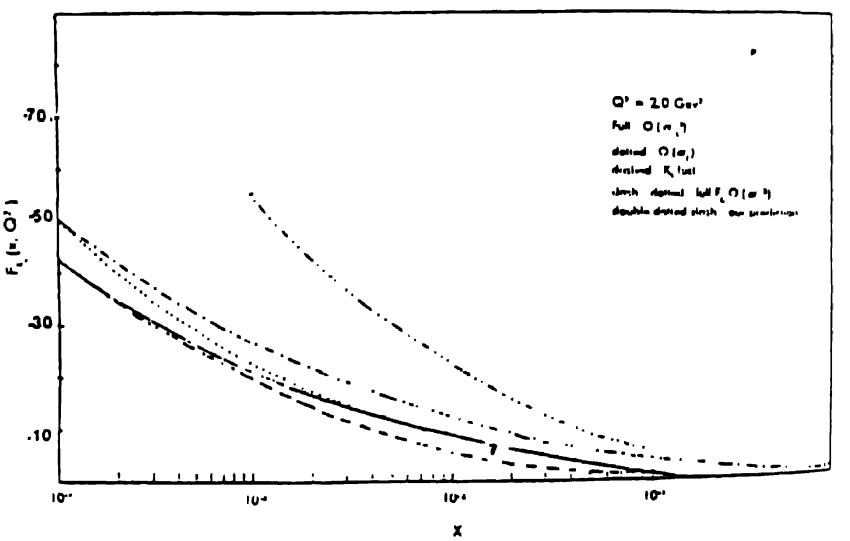

Figure 4. Comparison of F_L using (29) with the prediction of collinear [19] and k_T factorisation [21] approaches.

found to be higher than those of [19] and [21]. The difference increases as x decreases. However, as the cross-over of gluon distribution (29) with LO-GRV [22] occurs in the range $x \sim 10^{-1} - 10^{-2}$ for $Q^2 \sim 20$ GeV^2, the prediction may not be reliable for $x \leq 10^{-2}$.

3.2. Measuring the Gluon density directly from structure function :

Instead of F_L, a direct relation between $F_2(x, Q^2)$ and the gluon distribution $G(x, Q^2)$ will be more interesting from experimental point of view. Prytz [23] has initiated such a programme of study.

Using Taylor expansion approximation of GLAP equation [12], one obtains [23]

$$\frac{dF_2(x)}{d\ln Q^2} \approx \frac{\alpha_s}{4\pi}\frac{20}{9}G(2x). \tag{30}$$

The method has later been extended [24] to include the NLO corrections as well :

$$\frac{dF_2(x, Q^2)}{d\ln Q^2} = G(2x)\frac{20}{9}\frac{\alpha_s}{4\pi}\left[\frac{2}{3} + \frac{\alpha_s}{4\pi}3.58\right] + \left(\frac{\alpha_s}{4\pi}\right)^2\frac{20}{9}N(x, Q^2), \tag{31}$$

where $N(x, Q^2)$ is given explicitly [24]. The result for four flavour in the $\overline{MS}$ scheme explicitly yields [25]

$$G(x, Q^2) = \frac{dF_2(x/2, Q^2)/d\ln Q^2}{(40/27 + 7.96\alpha_s/4\pi)(\alpha_s/4\pi)} - \frac{(20/9)(\alpha_s/4\pi)N(x/2, Q^2)}{40/27 + 7.96\alpha_s/4\pi}. \tag{32}$$

An alternative method of extracting gluon density was proposed by Ellis Kunszt and Levin (EKL) [26].

In the EKL method [26], the gluon momentum density and F_2 are assumed to behave as $x^{-\omega_0}$, which leads to the following form for the scaling violation of F_2 :

$$\frac{d\Sigma}{d\ln Q^2} = P^{FF}(\omega_0)\sum(x, Q^2) + P^{FG}(\omega_0)g(x, Q^2) \tag{33}$$

with

$$\sum(x, Q^2) = \frac{1}{\langle e_q^2\rangle}\frac{F_2(x, Q^2)}{x}, \tag{34}$$

where $\langle e_q^2\rangle$ is the average of the squares of the quark charges ($\frac{5}{18}$ for four flavours). The non-singlet contributions are neglected. The evolution kernels P^{FF} and P^{FG} are expanded upto third order in α_s (NNL)

$$P^{FF}(\omega_0) = \alpha_s P_0^{FF} + \alpha_s^2 P_1^{FF} + \alpha_s^3 P_2^{FF}, \tag{35}$$

$$P^{FG}(\omega_0) = \alpha_s P_0^{FG} + \alpha_s^2 P_1^{FG} + \alpha_s^3 P_2^{FG}. \tag{36}$$

The LO and NLO-results are obtained by keeping in (35) and (36) the terms upto $O(\alpha_s)$ and $O(\alpha_s^2)$ respectively. The coefficients P_i^{FF} and P_i^{FG} depend on the parameter ω_0

and are tabulated in [26] for a range of ω_0 values. The actual value of ω_0 must be extracted from data.

In contrast to the Prytz method [23,24], quark contribution is included in the EKL method (33). The expression for the gluon momentum density for four flavours is

$$G(x, Q^2) = \frac{18/5}{P^{FG}(\omega_0)}\left[\frac{dF_2(x, Q^2)}{d\ln Q^2} - P^{FF}(\omega_0)F_2(x, Q^2)\right]. \qquad (37)$$

In the EKL method, in contrast to the Prytz method, the gluon density at x is calculated using the structure function F_2 and its logarithmic slope at the same value of x.

Figure 5 compares the results of Prytz [23] and EKL [26] methods, with that of the LO global GLAP fit [25] at $Q^2 = 20$ GeV^2. The results are consistent among each other.

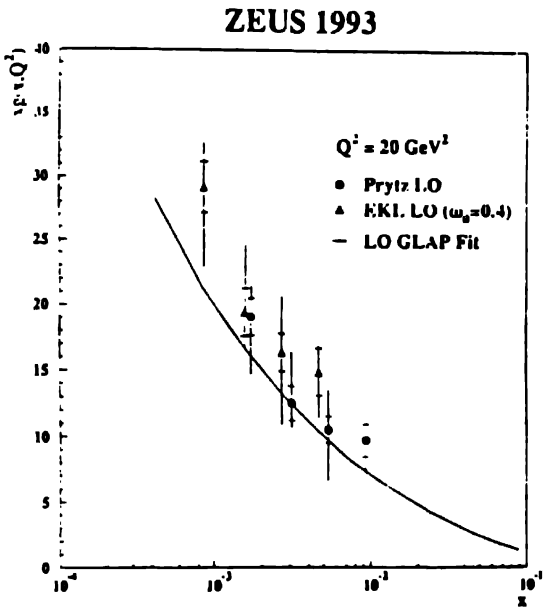

Figure 5. Gluon momentum density as a function of x at $Q^2 = 20$ GeV^2 determined from the ZEUS data using the method of Prytz [23] and EKL [26]. Solid line is the LO GLAP fit.

Figure 6 shows the gluon momentum density obtained in NLO. Good agreement between the results of the three methods is observed. The shaded band in Figure 6 indicates the uncertainity of the gluon density from the global GLAP fit as estimated by adding the statistical and systematic errors in quadrature.

A relation alternative to (30) have also been suggested recently [27] which reads

$$\frac{dF_2(x,Q^2)}{d\ln Q^2} = \frac{5\alpha_s}{9\pi}\frac{3}{4}G(4x/3) \tag{38}$$

The difference arises due to the choice of the expansion point of $G(\frac{x}{1-z}, Q^2)$ occurred in the GLAP equation [12].

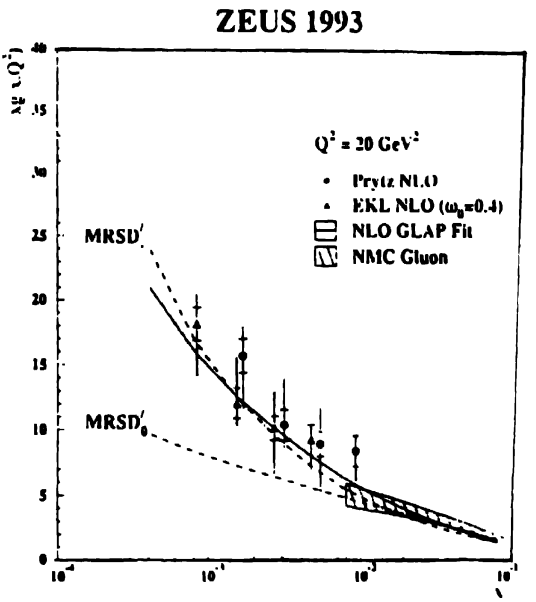

Figure 6. The gluon momentum density as a function of x at Q^2 = 20 GeV^2 determined from the ZEUS data using the methods of Prytz [24] and EKL [26] in the next to leading order. The solid line shows the result of the NLO GLAP global fit. It also shows the gluon distribution (hatched region) determined by the NMC experiment.

Gay Ducati and Goncalves [28] later obtained the expansion of the gluon distribution $G(\frac{x}{1-z})$ at an arbitrary point $z = \alpha$. Retainig terms only upto the first derivative in the expansion, they get in the limit $x \to 0$.

$$G\left[\frac{x}{1-\alpha}\left(\frac{3}{2}-\alpha\right)\right] \quad \frac{9\pi}{5\alpha_s}\frac{3}{2}\frac{dF_2(x,Q^2)}{d\ln Q^2} \tag{39}$$

This reduces to Prytz relation (30) for $\alpha = \frac{1}{2}$ while for $\alpha = 0$, it yields

$$\frac{dF_2(x,Q^2)}{d\ln Q^2} = \frac{5\alpha_s}{9\pi}\frac{3}{2}G\left(\frac{3}{2}x\right) \tag{40}$$

which is the corrected version of (38).

Recently Kotikov and Parente [28] present a set of formulæ to extract $F_L(x, Q^2)$ from $F_2(x, Q^2)$ and $\frac{dF_2(x, Q^2)}{d \ln Q^2}$ directly. Assuming $x^{-\delta}$ behaviour of the parton densities at low x, they obtain the following formula for $N_f = 4$ $\left(\alpha = \alpha_s (Q^2)/_{4\pi}\right)$:

$$F_L(x, Q^2) = \frac{1}{1 + 30\alpha\left(\frac{1}{\delta} - \frac{116}{45}\right)}\left[\frac{dF_2(x, Q^2)}{d \ln Q^2} + \frac{8}{3}\alpha F_2(x, Q^2)\right] \quad (41)$$

which will be useful in extracting longitudinal structure function directly from the structure function and its Q^2 derivative, instead of gluon distribution as (28).

4. Spin structure functions

Hadronic tensor $W_{\mu\nu}$ defined in deep inelastic lepton nucleon scattering has two spin structure functions g_1 and g_2 [29] :

$$\begin{aligned} W_{\mu\nu}(p, q) &= \int d^4 x e^{iqx} \langle p, s|\left[J_\mu(x), J_\nu(x)\right]|p, s\rangle \\ &= -g_{\mu\nu} F_1 + \frac{p_\mu p_\nu}{p.q} F_2 + \frac{iM_p}{p.q} e_{\mu\nu\alpha\beta} q^\alpha \\ &\times \left[s^\beta g_1 + \frac{p.qs^\beta - s.qp^\beta}{p.q} g_2\right] \end{aligned} \quad (42)$$

where s^α is the spin of the nucleon and other symbols have usual meaning. For longitudinally polarised beam and target, one measures the longitudinally polarised asymmetries

$$A_L = \frac{\mu\uparrow p\downarrow - \mu\uparrow p\uparrow}{\mu\uparrow p\downarrow + \mu\uparrow p\uparrow} \approx \frac{g_1^p(x, Q^2)}{F_1(x, Q^2)}, \quad (43)$$

and

$$W^{\parallel} = \pm\left[g_1 - \left(\frac{2xM_p}{Q}\right)^2 g_2\right] \approx \pm g_1. \quad (44)$$

For transversely polarised nucleon with polarisation perpendicular to the beam direction, the corresponding polarised asymmetry is

$$W^{\perp} = \pm\frac{2xM_p}{Q}(g_1 + g_2). \quad (45)$$

Conventionally, g_1 is called longitudinal spin structure function while g_2 is called the transverse structure function. g_1 has the interpretation of incoherent sum of parton probabilities

$$g_1(x, Q^2) = \frac{1}{2}\sum\nolimits_q e_q^2\left[\Delta q(x, Q^2) + \Delta\bar{q}(x, Q^2)\right], \quad (46)$$

where $\Delta q = q\uparrow - q\downarrow$. On the other hand, g_2 has no such simple partonic interpretation. It differs from zero because of the masses and the transverse momenta of the quarks. It has a

unique leading order sensitivity to twist-3 operators, *i.e.* quark gluon correlation effects in QCD. Thus g_2 will be a unique probe of higher twist effects [30].

In general, g_2 can be written as the sum of a contribution g_2^{WW}, directly calculable from g_1 [31] and a purely twist-3 term $\bar{g}_2$ [30]

$$g_2(x, Q^2) = g_2^{WW}(x, Q^2) + \bar{g}_2(x, Q^2) \tag{47}$$

with
$$g_2^{WW}(x, Q^2) = -g_1(x, Q^2) + \int_x^1 g_1(t, Q^2)\frac{dt}{t}. \tag{48}$$

Eq. (48) is called Wandzura-Wilczek relation.

A sum rule for g_2

$$\int_0^1 g_2(x, Q^2)dx = 0 \tag{49}$$

was derived by Burkhart and Cottingham [32] using Regge Theory. It has been regarded as a consequence of conservation of angular momentum [33]. At present, the validity of the derivation of the sum rule is in question [30,34] and it is clearly important to test it experimentally. SMC [35] have reported measurement of spin structure function g_2 as well as the asymmetry A_2 defined as

$$A_2 = \frac{2Mx}{\sqrt{Q^2}F_1}(g_1 + g_2). \tag{50}$$

Results of g_2^{WW} has also been summarised by SMC [35] as shown in Table 1.

Table 1. Results on the spin asymmetry A_2 and the structure functions g_2 and g_2^{WW} as reported in [35].

x interval	$\langle x \rangle$	$\langle Q^2\,(\mathrm{GeV}^2) \rangle$	A_2	g_2	g_2^{WW}
0.006 – 0.015	0.010	1.4	0.002 ± 0.083	1.2 ± 61	0.73 ± 0.10
0.015 – 0.050	0.026	2.7	0.041 ± 0.066	7.0 ± 12	0.47 ± 0.09
0.050 – 0.150	0.080	5.8	0.017 ± 0.091	0.2 ± 2.9	0.15 ± 0.02
0.150 – 0.600	0.226	11.8	0.149 ± 0.156	0.5 ± 0.8	−0.10 ± 0.02

E143 Collaboration [36] has measured structure functions g_2^p and g_2^d over the range $0.03 < x < 0.8$ and $1.3 < Q^2 < 10$ (GeV/c)^2, Figure 7. In the same figure the twist-2 g_2^{WW} calculation is shown using $g_1(x, Q^2)$ evaluated from a fit to world data [37] of asymmetry and assuming negligible higher twist contributions. Also shown are bag model predictions [38,39]. At high x, the results for g_2^p indicates a negative trend consistent with the expectation for g_2^{WW}. By extracting the quantity $\bar{g}_2(x, Q^2) = g_2(x, Q^2) - g_2^{WW}(x, Q^2)$, one looks for possible quark mass and higher twist effects. This can be seen from the difference between the data and the solid line in Figure 7. Within

the experimental uncertainity, the data are consistent with $\bar{g}_2$ being zero, but also $\bar{g}_2$ being of the same order of magnitude as g_2^{WW}

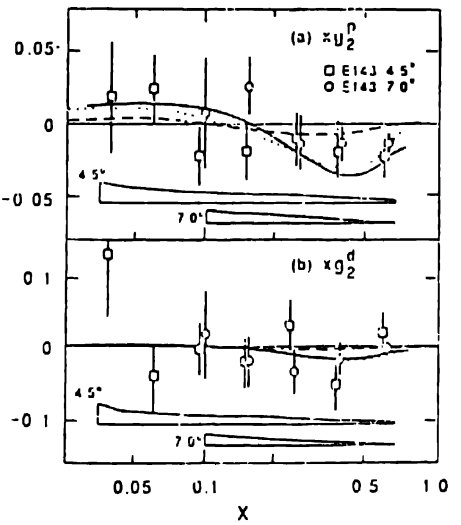

Figure 7. Measurement of (a) $x g_2^p$ and (b) $x g_2^d$ from E143 experiment [36]

E143 Collaboration [37] has also evaluated the integrals :

$$\int_{0.03}^{1} g_2^p(x)dx = -0.013 \pm 0.028 \cdot \tag{51}$$

$$\int_{0.03}^{1} g_2^d(x)dx = -0.033 \pm 0.082 \cdot \tag{52}$$

These results are consistent with zero and conforms to the expectation of sum rule (49).

More recently [40], results are reported from the HERMES experiment at HERA, on a measurement of the neutron spin structure function $g_1^n(x, Q^2)$ using 27.5 GeV longitudinally polarised positrons incident on a polarised ^{3}He target. The data cover the kinematic range $0.023 < x < 0.6$ and $1\ (\text{GeV}/c)^2 < Q^2 < 15\ (\text{GeV}/c)^2$. Evaluating at a fixed Q^2 of 2.5 $(\text{GeV}/c)^2$, experiment reports

$$\int_{0.023}^{0.6} g_1^n(x)dx = -0.034 \pm 0.013\,(stat) \pm 0.005\,(syst). \tag{53}$$

Assuming Regge behaviour at low x, the first moment comes out to be

$$\Gamma_1^n = \int_0^1 g_1^n(x)dx = -0.037 \pm 0.013\,(stat) \pm 0.005\,(syst) \pm 0.006\,(extrapol) \tag{54}$$

5. Diffractive structure function

The observation of "diffractive" deep inelastic scattering (DDIS) events with a large rapidity gap [41] has opened up a new field on structure functions in the last few years.

While in the non-diffractive deep inelastic scattering (DIS) where a virtual photon probes a parton (Figure 8), in diffractive deep inelastic scattering (DDIS), a virtual photon

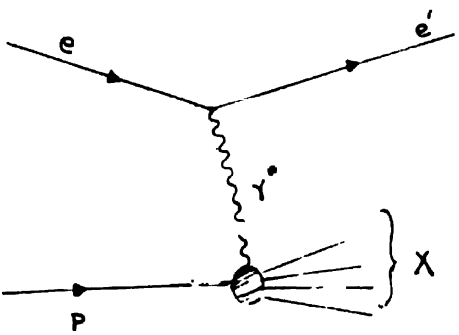

Figure 8. Usual deep inelastic $e + p \to e + X$

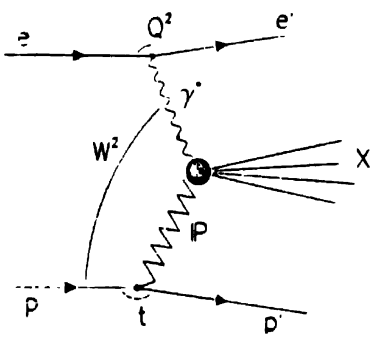

Figure 9. Diffractive deep inelastic scattering $e + p \to e + P + X$

probes a colour neutral object emitted from the target proton (Figure 9). This colour neutral object is called "Pomeron".

In usual DIS, the standard kinematic variables are

$$x = \frac{Q^2}{2p.q}, \quad y = \frac{p.q}{p.k},$$

$$W^2 = (p+q)^2, \quad Q^2 = -q^2, \tag{55}$$

where P, k, k' and $q = k - k'$ are the four momenta of the proton, incident lepton, final lepton and the virtual photon.

In DDIS, the proton remnant emerges with momentum P'. As a result, one introduces the additional kinematic variables [34]

$$x_P = \frac{q.(P-P')}{q.P}, \quad \beta = \frac{Q^2}{2q.(P-P')}$$

and $$t = (P-P')^2 \tag{56}$$

besides $$x = \frac{Q^2}{2P.q} = x_P\beta.$$

Furthermore

$$x_P = \frac{Q^2 + Mx^2 - t}{Q^2 + W^2 - M_p^2}, \quad \beta = \frac{Q^2}{Q^2 + M_X^2 - t}, \tag{57}$$

where $M_X^2 = -Q^2 + (P-P')^2$. For

$$M_p^2 \ll Q^2, W^2, \quad |t| \ll Q^2, M_X^2 \tag{58}$$

$$x_P \approx \frac{M_X^2 + Q^2}{W^2 + Q^2} \tag{59}$$

and $$\beta \approx \frac{Q^2}{M_X^2 + Q^2} \equiv \frac{x}{x_P}. \tag{60}$$

In this limit [34],

$x_P \equiv$ Fraction of the Proton's four momentum transferred to the Pomeron and

$\beta \equiv$ Fraction of the Pomeron's four momentum carried by the quark entering the hard process.

The DDIS cross section for the process $e\,p \to e + X + p$ is given by

$$\frac{d\sigma(\beta, Q^2, x_P)}{d\beta\, dQ^2\, dx\, dx_P} = \frac{2\pi\alpha^2}{\beta Q^4}\left[1 + (1-y)^2\right] F_2^{D(3)}(\beta, Q^2, x_P), \tag{61}$$

where $F_2^{D(3)}(\beta, Q^2, x_P)$ is called the diffractive structure function, integrated over the variable t. The unintegrated version is denoted by $F_2^{D(4)}(\beta, t, Q^2, x_P)$.

The main experimental features of $F_2^{D(3)}$ are :

(a) x_P dependence :

This is shown in Figure 10 which is in the range $2 \times 10^{-4} < x_P < 2 \times 10^{-2}$.

Fit to the ZEUS data [16] yields

$$F_2^{D(3)} \sim \left(\frac{1}{x_P}\right)^a \tag{62}$$

with $$a = 1.46 \pm 0.04 \pm 0.08. \tag{63}$$

Corresponding analysis of H1 experiment [16] fixes a at

$$a = 1.19 \pm 0.06 \pm 0.07. \tag{64}$$

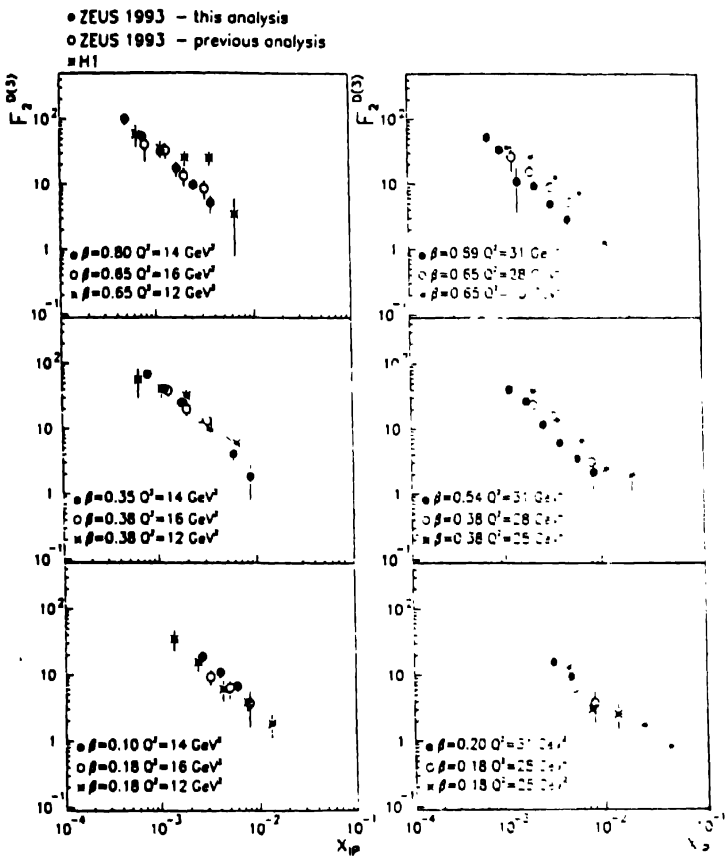

Figure 10. The diffractive structure function $F_2^{D(3)}$ (solid line) as a function [16] of x_P for various values of β and Q^2. Open dots and stars are from previous measurements.

(b) β dependence :

It is shown in Figure 11. The largest range of β is covered in the experiment is at x_P = 0.003. Figure 11 shows that $F_2^{D(3)}$ rises as β decreases, which is expected from QCD evolution of parton densities of proton.

The unintegrated diffractive structure function $F_2^{D(4)}$ and the Pomeron structure function F_2^P are related *via* the Factorisation ansatz [42]

$$F_2^{D(4)}(x_P, \beta, t, Q^2) \Leftrightarrow f_{P/P}(x_P, t) F_2^P(\beta, Q^2) \tag{65}$$

where $f_{p/p}(x_p, t)$ is the flux factor describing the flux of Pomerons in the proton, which can be extracted from hadron-hadron scattering assuming universality of the proton flux.

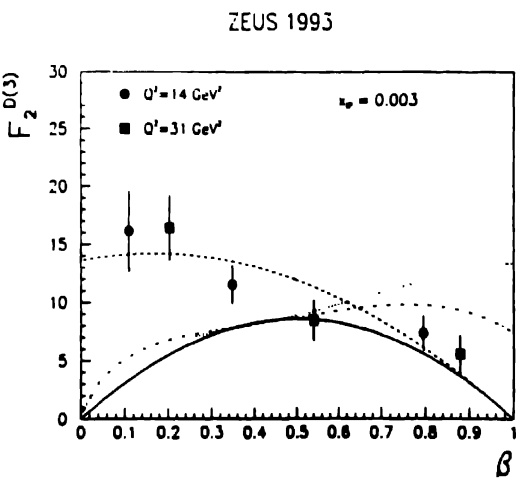

Figure 11. The diffractive structure function $F_2^{D(3)}$ as a function of β at $x_{\mathbb{P}}$ = 0.003 at Q^2 = 14 and 31 GeV^2. The full line, dashed line, dashed dotted and dotted lines are model predictions discussed in [16].

The Pomeron structure function has the parton decomposition

$$F_2^{\mathbb{P}}(\beta, Q^2) = \sum_i e_{q_i}^2 \beta\left[f_{q_i}(\beta, Q^2) + \bar{f}_{q_i}(\beta, Q^2)\right]. \tag{66}$$

where $f_{q_i}(\beta, Q^2)\left(\bar{f}_{q_i}(\beta, Q^2)\right)$ is the probability of finding a parton (antiparton) of flavour q with momentum fraction β inside the Pomeron. For "hard Pomeron" and "soft Pomeron" they have simple forms [43]

$$\begin{aligned} F_2^{\mathbb{P}}(\beta, Q^2) &\sim \beta(1-\beta) \quad : \textit{ Hard Pomeron} \\ &\sim (1-\beta)^5 \quad : \textit{ Soft Pomeron} \end{aligned} \tag{67}$$

Q^2 dependence of $F_2^{\mathbb{P}}$ is expected to be weak and is neglected.

Parametrizations for Pomeron flux factors are also reported in the literature. The Ingelmen-Schlein form of the flux factor [42] is parametrized by a fit to UA4 data [43]

$$f_{\mathbb{P}}(x_{\mathbb{P}}, t) = \frac{1}{2}\frac{1}{2.3}\frac{1}{x_{\mathbb{P}}}\left[0.38\, e^{8t} + 0.424\, e^{3t}\right]. \tag{68}$$

On the other hand in the Donnachie-Landshoff model [44], the flux factor is

$$f_{\mathbb{P}}(x_{\mathbb{P}}, t) = \frac{9\beta_0^2}{4\pi^2} F_1(t^2)\, x_{\mathbb{P}}^{1-2\alpha_{\mathbb{P}}(t)}, \tag{69}$$

where $\beta_0 = 1.8$ GeV^{-1} and $F_1(t)$ is elastic form factor of the proton.

The Pomeron trajectory $\alpha_P(t)$ occurring in (69) obeys a linear relation :

$$\alpha_P(t) = \alpha_P(0) + \alpha'_P t. \tag{70}$$

Defining $\overline{\alpha}_P$ as $\alpha_P(t)$ averaged over t, the exponent a defined in (62) obeys the relation

$$\overline{\alpha}_P = \frac{a+1}{2} \tag{71}$$

From the W dependence of the diffractive cross section

$$\overline{\alpha}_P = 1.23 \pm 0.02\,(stat) \pm 0.04\,(syst) \tag{72}$$

which is in between the soft Pomeron $\overline{\alpha}_P \sim 1.05$ occurred in hadron-hadron collisions [44] and the hard or BFKL Pomeron (17) with $\overline{\alpha}_P \sim 1.5$.

6. Conclusion

With the start of the HERA experiments, a novel era in the investigation of the proton structure has began. The Double Asymptotic Scaling, methods of measurements of gluon and longitudinal structure functions, diffractive structure functions discussed in this talk are the topics which evolved mostly during the present-HERA years. Although the study of spin structure functions dates back to the sixties, experimental information on g_2 has become available only during last few years. Coming years with HERA, LHC and LEP ⊗ LHC will undoubtedly throw new light in the structure of the nucleon.

7. Acknowledgments

I gratefully acknowledge financial support from the Department of Science and Technology, Government of India. I also thank Abhijeet Das for helping me preparing the manuscript.

References

[1] N Pavel, DESY 95-147

[2] W J Stirling, hep-ph/9608411

[3] see for example, ZEUS Collaboration, DESY 96-018

[4] SMC Collaboration, D Adams *et al Phys. Lett.* **B336** 125 (1994)

[5] E143 Collaboration, K Abe *et al Phys. Rev. Lett.* **76** 587 (1996)

[6] A De Rujula, S L Glashow, H D Politzer, S B Trieman, F Wilczek and A Zee *Phys. Rev.* **D10** 1649 (1974)

[7] R D Ball and S Forte *Phys. Lett.* **B335** 77 (1994); *Phys. Lett.* **B336** 77 (1994)

[8] ZEUS Collaboration, *Phys. Lett.* **B316** 412 (1993), H1 Collaboration, *Nucl. Phys.* **B407** 515 (1993)

[9] H1 Collaboration, S Aid *et al Phys. Lett.* **B354** 494 (1995)

[10] R D Ball and S Forte *Proc. XXXV Cracow School of Theoretical Physics* (Zakopane, June 1995); CERN TH/95-323

[11] L V Gribov, E M-Levin and M G Ryskin *Phys. Rep.* **100** 1 (1983)

[12] G Altarelli and G Parisi *Nucl. Phys.* **B126** 298 (1977); V N Gribov and L N Lipatov *Sov. J. Nucl. Phys* **15** 438 (1972); L N Lipatov *Sov. J. Nucl. Phys.* **20** 94 (1975)

[13] H1 Collaboration, S Aid *et al* DESY 96-039 (1996)

[14] A De Roeck, M Klein and T Naumann DESY 96-063 (1996)

[15] W Buchmüller and D Haidt DESY 96-061 (1996)

[16] ZEUS Collaboration, M Derrick *et al* DESY 96-018; H1 Collaboration, S Aid *et al* DESY 96-039 (1996)

[17] E A Kureav, L N Lipatov and V S Fadin *Sov. Phys JETP* **45** 199 (1977), Ya Ya Balitsky and L N Lipatov *Sov. J. Nucl. Phys* **28** 822 (1978)

[18] A M Cooper Sarkar *et al. Z. Phys* **C39** 281 (1988)

[19] E B Zilstra and W L Van Neerven *Nucl. Phys.* **B383** 552 (1992)

[20] R Deka and D K Choudhury *Z. Phys.* **C75** 679 (1997)

[21] J Blümlein *Nucl Phys. B. Proc. Suppl.* **39 BC** 22 (1995)

[22] M Glück, E Reya and A Vogt *Z. Phys.* **C53** 127 (1997)

[23] K Prytz *Phys. Lett* **B311** 286 (1993)

[24] K Prytz *Phys. Lett.* **B332** 393 (1994)

[25] ZEUS Collaboration, M Derrick *et al. Phys. Lett* **B345** 576 (1995)

[26] R K Ellis, Z Kunszt and E M Levin *Nucl. Phys.* **B420** 517 (1994)

[27] K Bora and D K Choudhury *Phys. Lett.* **B354** 151 (1995)

[28] A V Kotikov and G Parente US-FT/19-96, hep-ph/9605207 (1996)

[29] See for example, F E Close in *'An Introduction to Quarks and Partons'* (New York Academic) (1979)

[30] R L Jaffe *Comments Nucl. Part. Phys.* **19** 239 (1992)

[31] S Wandzura and F Wilczek *Phys. Lett.* **B72** 195 (1977)

[32] H Burkhart and W N Cottingham *Ann. Phys.* **56** 453 (1970)

[33] R P Feynman in *'Photon-Hadron Interactions'* (New York : Benjamin) (1972)

[34] L Mankiewicz and A Schäfer *Phys Lett.* **B265** 167 (1991)

[35] SMC Collaboration, D Adams *et al. Phys Lett* **B336** 125 (1994)

[36] E143 Collaboration, K Abe *et al. Phys. Rev. Lett* **76** 587 (1996)

[37] E143 Collaboration, K Abe *et al. Phys. Lett.* **B364** 61 (1994)

[38] X Song and J S McCarthy *Phys Rev.* **D49** 3169 (1994).

[39] M Stratmann *Z. Phys.* **C60** 763 (1993)

[40] HERMES Collaboration, K Acherstaff *et al. Phys Lett* **B404** 383 (1997)

[41] ZEUS Collaboration, M Derrick *et al. Phys. Lett.* **B315** 481 (1993); **B332** 228 (1994), **B338** 483 (1994); H1 Collaboration, T Ahmed *et al. Nucl. Phys* **B429** 477 (1994)

[42] G Ingelman and P Schlein *Phys. Lett.* **B152** 256 (1985)

[43] UA4 Collaboration, M Bozzo *et al. Phys. Lett* **B136** 217 (1984)

[44] A Donnachie and P V Landshoff *Nucl. Phys* **B303** 634 (1988); *Phys. Lett* **B285** 172 (1992)